American Journal of Energy Engineering
2026, Vol. 14, No. 4, pp. 179–191
https://doi.org/10.11648/j.ajee.20261404.12

Research Article

Rule-Based Operation of a Grid-Connected Hybrid Power System in Coastal Bangladesh

Fahim Faisal[1], Cheng Peng[1,*], Md Shivly Mahmood[2]

[1]College of Intelligent System Science and Engineering, Harbin Engineering University, Harbin, China
[2]College of Nuclear Science and Technology, Harbin Engineering University, Harbin, China

Abstract

Coastal communities in Bangladesh, such as Teknaf in Cox's Bazar, suffer from severe energy insecurity due to a fossil-fuel-dominated grid, long transmission lines, and chronic load shedding. This study aims to design and evaluate a grid-connected hybrid power system to improve local energy reliability, reduce grid dependence, and lower carbon emissions. A 24-hour hourly simulation was conducted using real commercial components: five 95 kW wind turbines (475 kW total), a 78.12 kWp bifacial solar PV array, a 128 kWh $LiFePO_4$ battery, a 100 kVA diesel generator, and bidirectional grid exchange. A transparent, rule-based energy management strategy with four time-of-day operating modules was developed to coordinate the sources and serve a consumer load with a 70-kW evening peak. The simulation results show that renewable generation (1,150 kWh/day) exceeded the consumer demand (929 kWh/day). This reduced gross grid imports by 41.3% and net grid purchase, along with associated CO_2 emissions, by 84.5% compared to a CG-only system. However, the temporal mismatch between renewable generation and the evening peak meant that the 128-kWh battery only reduced the peak grid demand from 70 kW to 67.5 kW. Sensitivity analysis identified wind speed and battery capacity as the most dominant design parameters.

Keywords

Hybrid Power System, Renewable Energy Sources, Wind-PV-Battery, Grid Interaction, Rule-based Control, CO_2 Emission Reduction

1. Introduction

Hybrid renewable energy systems (HRESs) that combine solar photovoltaic (PV) generation, wind turbines, battery energy storage and conventional backup are now a mainstream route to cleaner and more reliable electricity supply [1, 2]. Their main technical challenge is the variability of solar and wind output, which must be balanced against demand through storage sizing and energy management [3]. Recent reviews show that storage, control strategy and grid interaction largely determine whether a hybrid system delivers its expected reliability and stability benefits [2-4].

Bangladesh is a strong case for such systems. Its generation mix remains heavily dependent on fossil fuels: renewables supplied only about 3.54% of a 28,132 MW total generation capacity, and grid-connected wind capacity was just 63 MW, despite a national target of 40% renewable electricity by 2041 [5]. The southern coastal belt, which includes Cox's Bazar

*Correspondence: Cheng Peng (chengpeng040703@aliyun.com)

Received: 6 October 2026; **Accepted:** 26 October 2026; **Published:** 10 November 2026

Copyright: © The Author(s), 2026. Published by Science Publishing Group. This is an **Open Access** article, distributed under the terms of the Creative Commons Attribution 4.0 License (http://creativecommons.org/licenses/by/4.0/), which permits unrestricted use, distribution and reproduction in any medium, provided the original work is properly cited.

District and the Teknaf peninsula (Figure 1), has the country's best wind resource, with average speeds of roughly 5.5-7.2 m/s at 100 m hub height [5]. At lower heights the resource is more modest; for example, the highest annual mean speed among 50 surveyed locations was 4.89 m/s at 50 m, recorded at Sandwip [6]. Coastal sites have nonetheless been shown to suit cost-effective generation at 30-40 m tower heights [7], and GIS-based siting studies have mapped large areas of coastal Bangladesh suitable for wind development [8].

A growing body of work has applied techno-economic optimization, to hybrid systems in coastal and island Bangladesh. Studies have covered a solar-wind system at Patenga Sea Beach [9], six off-grid and on-grid configurations for Kunder Char [10], large-scale electrification of Bhasan Char [11], a smart PV-wind-battery-grid microgrid with demand response for Hatiya Island [12], and a hydrogen-assisted off-grid microgrid for Char Ishwar, Noakhali [13]. In Cox's Bazar itself, recent work evaluated a hybrid EV charging station and showed that aligning demand with solar hours reduces cost and emissions [14]. Related studies have added dynamic stability assessment to rural microgrid design [15] and compared battery chemistries, including $LiFePO_4$, for off-grid hybrid systems [16].

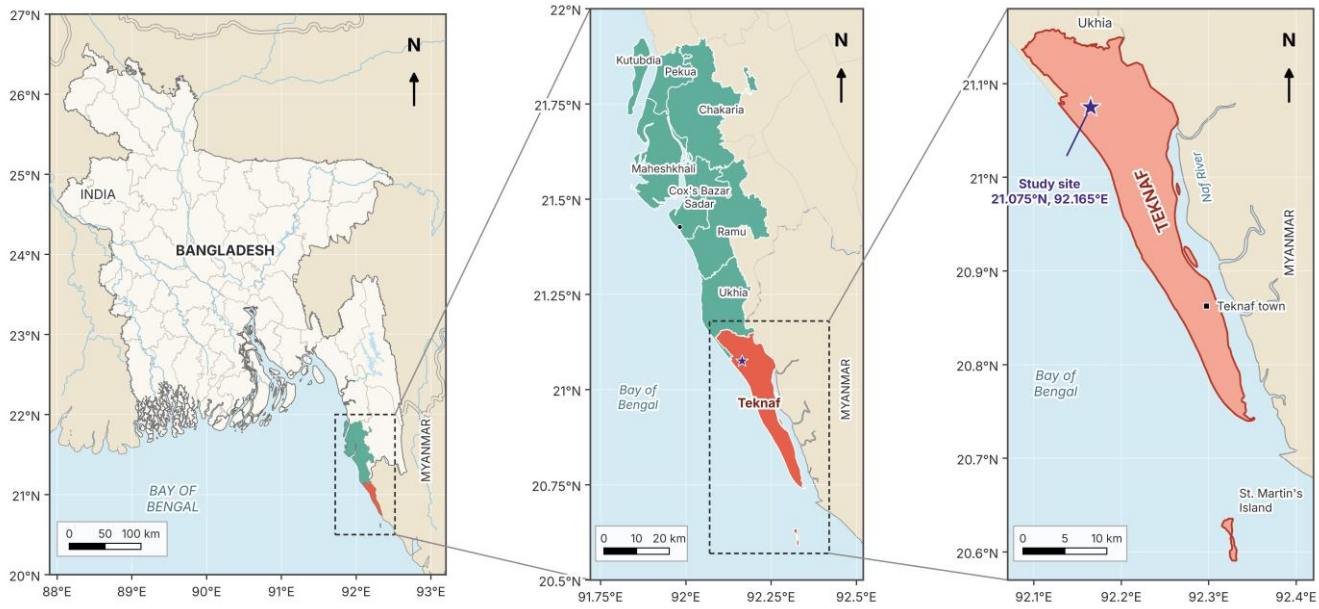


Figure 1. *Location of the study site in Teknaf, Cox's Bazar, Bangladesh.*

In parallel, rule-based energy management systems (EMSs) have been developed to coordinate generation, storage and the grid in a transparent and practical way. Recent proposals include modular rule-based EMSs that adapt to different microgrid configurations in grid-connected and islanded modes [17], improved rule-based schemes for coordinating batteries in community microgrids [18], rule-based peak-shaving control for grid-connected PV-battery communities [19], and rule-based EMSs combined with metaheuristic sizing [20].

Despite this progress, three gaps remain. First, most coastal Bangladesh studies focus on off-grid island electrification and report annual economic indicators, while grid-connected community systems that both import and export power receive less attention [9-13]. Second, operating strategy is often left to software defaults, so the hour-by-hour interaction between wind, solar, battery, generator and grid is rarely made explicit or reproducible [17-19]. Third, few studies model a specific Teknaf community load using real commercial component specifications, or examine how a backup generator and battery maintain supply during grid outages, which remain common in the region. To address these gaps, this paper presents a grid-connected hybrid community power system installed at Teknaf, Cox's Bazar, Bangladesh.

2. Materials and Methods

2.1. Study Area and System Design Philosophy

The hybrid community power system described in this study was installed to meet the electricity demand of a coastal community in Teknaf, Cox's Bazar, Bangladesh. Teknaf was selected because of its abundant renewable energy resources. The coastal area experiences a typical sea breeze pattern, with average wind speeds ranging from 4.5 to 5.5 m/s at 30-40 m height, and receives an average of 4.5 peak sun hours per day, making it suitable for both wind and solar PV generation.

The system architecture combines wind turbines, solar photovoltaic panels, battery energy storage, a backup diesel gen-

erator, and a grid connection to form a resilient and sustainable power supply network. The primary design objective was to maximize the utilization of renewable energy sources while ensuring reliable power delivery during periods of low renewable generation and grid outages. The total renewable generation capacity is 553.12 kW, comprising 475 kW from wind turbines and 78.12 kWp from solar PV panels. This capacity exceeds the community's peak demand of 70 kW by a factor of approximately 7.9, ensuring sufficient generation during favorable conditions and enabling substantial energy export to the grid. Figure 2 presents the overall system architecture.

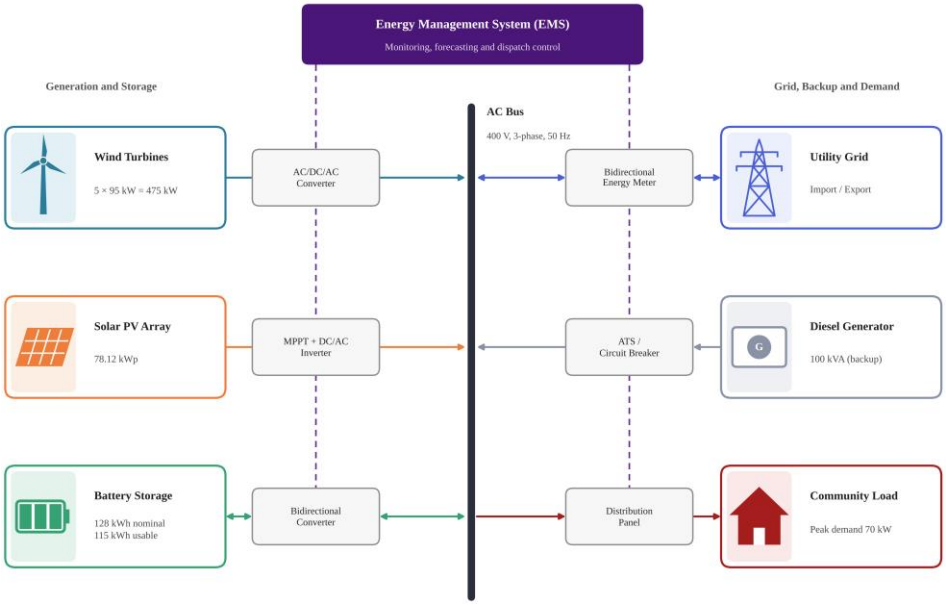


Figure 2. *Overall system architecture of the hybrid community power system.*

2.2. User Load Profile

The user load profile was developed based on a connected load of 100 kW and a demand factor of 0.7, yielding a peak demand of 70 kW. The demand factor accounts for the fact that not all connected loads operate simultaneously at their rated capacity, a standard assumption in power system planning. The daily energy consumption is 929 kWh, with a load factor of 55 percent. The load profile exhibits a typical residential-commercial pattern, with minimum demand during early morning hours and peak demand in the evening at 19:00.

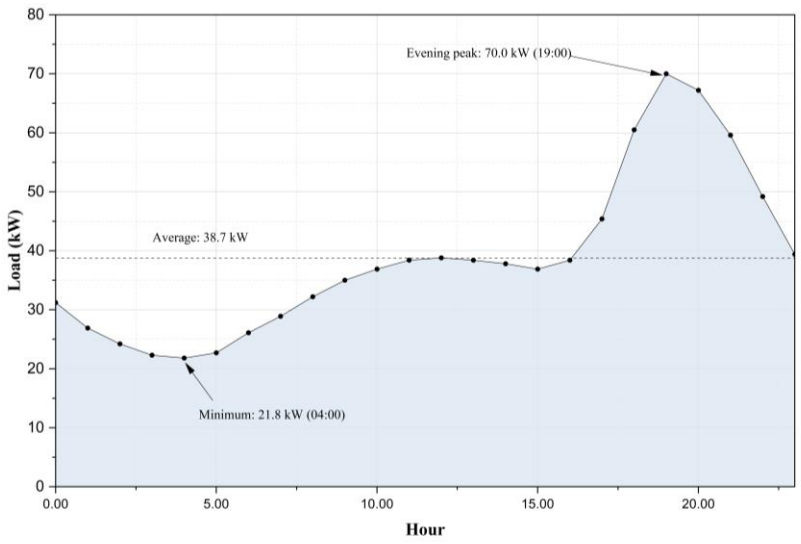


Figure 3. *Daily Load Curve.*

Figure 3 presents the hourly load profile. The load rises gradually from a minimum of 21.8 kW at 04:00 to a daytime plateau of approximately 38 kW between 10:00 and 16:00. A sharp increase occurs after 17:00, reaching the peak of 70 kW at 19:00, followed by a gradual decline through the evening and night. This profile is characteristic of coastal communities in Bangladesh, where evening lighting, cooling, and commercial activities drive peak demand.

2.3. Wind Based Power Generation Model

2.3.1. Turbine Specifications

Table 1. Wind turbine specifications (XANT M-24).

Parameter	Specification
Model	XANT M-24
Rated Power	95 kW
Rotor Diameter	24 m
Swept Area	452 m ²
Cut-in Wind Speed	3.0 m/s
Rated Wind Speed	11-12 m/s
Cut-out Wind Speed	25 m/s
Number of Units	5
Total Installed Capacity	475 kW

The wind-based power generation model is based on the XANT M-24 wind turbine (WT), a 95-kW rated machine with a 24 m rotor diameter. Five such WTs are installed, providing a total installed capacity of 475 kW. The turbine has a cut-in wind speed of 3.0 m/s and reaches its rated power at approximately 11-12 m/s. Table 1 presents the technical specifications of the wind turbine.

2.3.2. Wind Power Calculation

The power output from WT at each hour was calculated using the standard wind power equation:

$$P = \frac{1}{2}\rho A v^3 C_p \quad (1)$$

where $\rho$is the air density, A is the rotor swept area, v is the wind speed, and C_p is the power coefficient, assumed to be 0.40 for this analysis. The theoretical model was chosen because the manufacturer's certified power curve was not available for this specific WT model at the time of the study.

2.4. Solar PV based Power Generation Model

2.4.1. Panel Specifications

Table 2. Solar PV panel specifications (Jinko Tiger Neo 620 W).

Parameter	Specification
Model	JKM620N-78HL4-BDV
Cell Type	N-type TOPCon, bifacial, dual glass
Rated Power	620 W
Efficiency	22.2%
V_{mp}/I_{mp}	45.6 V/13.6 A
V_{oc}/I_{sc}	55.5 V/14.3 A
Temp. Coefficient (Pmax)	-0.29% / ℃
Dimensions	2465×1134×30 mm
Number of Panels	126
Total Installed Capacity	78.12 kWp

The solar PV generation model is based on the Jinko Tiger Neo 620 W (JKM620N-78HL4-BDV) module, a bifacial N-type TOPCon panel with an efficiency of approximately 22.2 percent. A total of 126 panels is installed, providing an installed capacity of 78.12 kWp. The panel has a temperature coefficient of -0.29 percent per degree Celsius, which was accounted for in the output calculation. Table 2 presents the technical specifications of the solar PV panel.

2.4.2. Solar Power Calculation

The hourly power output was estimated using a typical solar radiation profile for coastal Bangladesh, with a peak of 850 W/m ²at solar noon. The output was calculated using the formula:

$$P_{PV} = P_{STC} \times \frac{G}{G_{STC}} \times [1 + \alpha(T_c - T_{STC})] \quad (2)$$

where $P_{STC}$is the rated power at standard test conditions, $G$is the actual solar radiation, $G_{STC}$is the standard test condition radiation, $\alpha$is the temperature coefficient, T_c is the cell temperature, and $T_{STC}$is the standard test condition temperature.

2.5. Battery Energy Storage System

The battery energy storage system was sized at 128-kWh nominal capacity using eight HiTHIUM HeroEE 16 units, each rated at 16 kWh. The battery chemistry is LiFePO4, which offers high cycle life, thermal stability, and safety. The

usable capacity was estimated at 115 kWh, assuming a depth of discharge of 90 percent. The round-trip efficiency was assumed to be 95 percent. Table 3 presents the technical specifications of the battery system.

Table 3. The solar radiation and corresponding electric power for the 126 panels array.

Parameter	Value
Model	HiTHIUM HeroEE 16
Chemistry	$LiFePO_4$ (LFP)
Nominal Voltage	51.2 V
Capacity per Unit	314 Ah / 16 kWh
Number of Units	8
Total Nominal Capacity	128 kWh
Usable Capacity (90% DoD)	115 kWh
Round-Trip Efficiency	95%
Cycle Life	11,000 cycles
Max Parallel Units	16
Operating Temperature	-10 ℃ to 55 ℃

The battery system was designed to charge during the midday surplus period (09:00-17:00) and discharge during the evening peak and night hours (18:00-08:00). Table 3 presents the technical specifications of the battery system. The battery management system was configured to maintain the state of charge (SOC) above 20 percent to protect battery life and ensure availability for emergency backup.

Table 4. Backup generator specifications.

Parameter	Specification
Rated Capacity	100 kVA / 80 kW
Voltage	415 V, 3-phase
Frequency	50 Hz
Power Factor	0.8
Speed	1500 RPM
Fuel Type	Diesel
Configuration	Silent/soundproof canopy
Control	ATS

2.6. Backup Generator

A 100 kVA diesel generator was included as the final layer of backup in the system. The generator is rated at 80 kW at a power factor of 0.8 and operates at 415 V, 3-phase, 50 Hz. It is equipped with an automatic transfer switch (ATS) that enables automatic startup during grid failure when the battery state of charge falls below 20 percent. Table 4 presents the generator specifications. The generator was sized to cover the community's peak demand of 70 kW with a margin for surge currents during motor starting and battery charging.

2.7. Grid Connection and Power Flow Convention

The system was designed to operate in parallel with the local grid, allowing both import and export of electricity. The grid connection is rated at 400 V, 3-phase, 50 Hz. In the power flow analysis, positive values indicate import from the grid, while negative values indicate export to the grid. The grid serves as a balancing mechanism, absorbing surplus renewable generation during midday and supplying power during evening peak hours when renewable generation is insufficient.

2.8. Proposed Hybrid Grid Management (HGM) and Operational Modules

The 24-hour operation was divided into four distinct modules based on the availability of renewable resources and the state of the battery. These modules are summarized in Table 5. Module M1 (22:00-05:00) represents the night base period, where neither solar nor wind generation is available, and the battery discharges to reduce grid import. Module M2 (06:00-08:00) represents the morning ramp period, where solar and wind generation begin to increase, and the battery continues to discharge. Module M3 (09:00-16:00) represents the midday surplus period, where both solar and wind generation are high, the battery charges, and excess power is exported to the grid. Module M4 (17:00-21:00) represents the evening peak period, where solar generation is zero, wind generation is low, and the battery discharges to meet peak demand.

Table 5. Operational modules for 24-hour system operation.

Module	Hours	Solar	Wind	Battery	Grid
M1	22:00-05:00	✗	✗	Discharge	Import
M2	06:00-08:00	✓ (low)	✓ (low)	Discharge	Import
M3	09:00-16:00	✓ (high)	✓ (high)	Charge	Export
M4	17:00-21:00	✗	✓ (low)	Discharge	Import

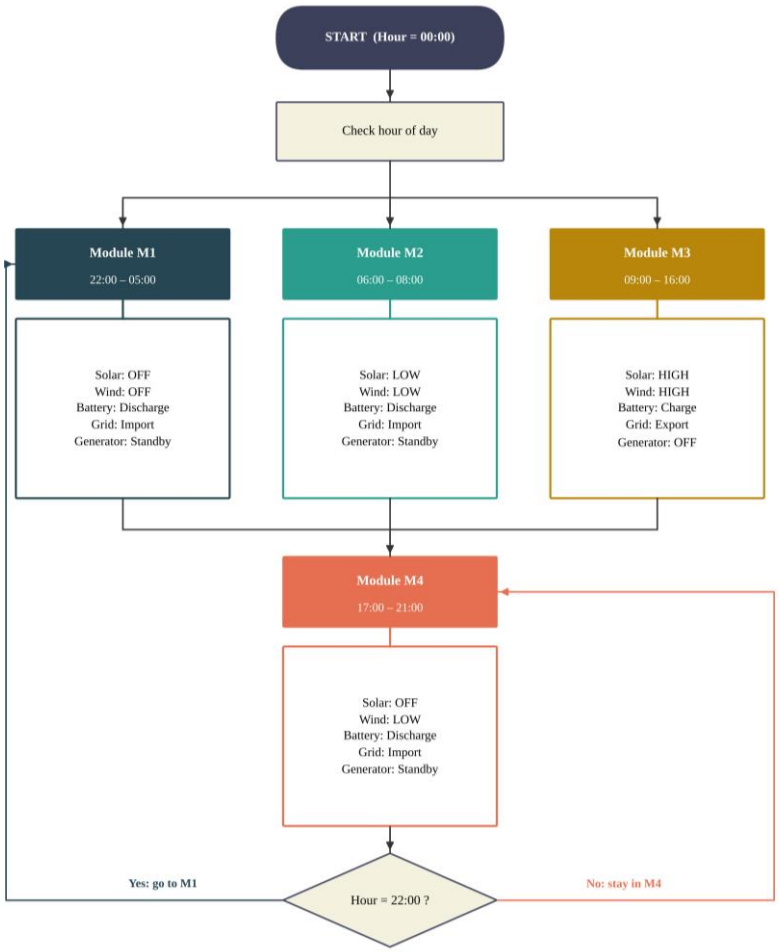


Figure 4. *State machine diagram of the four operational modules.*

Figure 4 presents a state machine diagram illustrating the transitions between these four operational modules. The transitions occur at fixed times of the day, ensuring deterministic and predictable system operation.

2.9. Economic and Environmental Parameters

The economic analysis was not included due to insufficient local pricing data. The environmental analysis used a grid emission factor of 0.65 kg CO_2 per kWh, which is a conservative average of recent estimates for Bangladesh [21, 22]. This factor was applied to the net grid import to estimate daily CO_2 emissions. The hybrid community power system proposed in this study was designed to meet the electricity demand of a coastal community in Teknaf, Cox's Bazar, Bangladesh. Teknaf was selected as the study location because of its abundant renewable energy resources. The coastal area experiences a typical sea breeze pattern, with average wind speeds ranging from 4.5 to 5.5 m/s at 30-40 m height, and receives an average of 4.5 peak sun hours per day, making it suitable for both wind and solar PV generation.

3. Results and Discussion

3.1. Overview of System Performance

The HGM system was evaluated over a 24-hour period to assess its technical and environmental performance. The results demonstrate that the system reliably meets the consumer's load demand while achieving a renewable share of approximately 84.5 percent. The total daily generation from wind and solar is 1,150 kWh, exceeding the total load of 929 kWh by 221 kWh. This surplus is exported to the grid, contributing to the economic viability of the system.

Table 6 presents the complete 24-hour power flow results, showing the load, wind generation, solar generation, total generation, grid interaction, and battery action for each hour. The results reveal a clear pattern of midday surplus and evening deficit, which is characteristic of systems with high solar penetration.

3.2. Wind Generation Analysis

The five XANT M-24 turbines generated a total of 785 kWh

over the 24-hour period. The peak output of 132.5 kW occurred at 13:00-14:00, when wind speeds reached 5.5 m/s. However, the wind farm produced zero power for 16 hours of the day, from 19:00 to 08:00, when wind speeds fell below the 3.0 m/s cut-in threshold. This zero-production period coincides with the community's evening peak demand, highlighting the need for battery storage and grid support.

The capacity factor of the wind farm is 6.9 percent, which is low compared to typical wind farm capacity factors of 25-40 percent. This low value reflects the modest wind resource at the study site, where average wind speeds are approximately 3.2 m/s at 10 m height. The results suggest that the XANT M-24 turbine, while suitable for low-wind sites, is still oversized for the Teknaf wind regime.

Table 6. Complete 24-hour power flow results.

Hour	Load (kW)	Wind (kW)	Solar (kW)	Total Gen (kW)	Grid (kW)	Battery Action
00:00	31.2	0.0	0.0	0.0	+31.2	Discharge*
01:00	26.9	0.0	0.0	0.0	+26.9	Discharge
02:00	24.2	0.0	0.0	0.0	+24.2	Discharge
03:00	22.3	0.0	0.0	0.0	+22.3	Discharge
04:00	21.8	0.0	0.0	0.0	+21.8	Discharge
05:00	22.7	0.0	0.0	0.0	+22.7	Discharge
06:00	26.1	0.0	1.0	1.0	+25.1	Discharge
07:00	28.9	0.0	9.5	9.5	+19.4	Discharge
08:00	32.2	2.5	22.1	24.6	+7.6	Discharge
09:00	35.0	34.0	34.7	68.7	-33.7	Charge
10:00	36.9	51.0	44.1	95.1	-58.2	Charge
11:00	38.4	72.5	50.4	122.9	-84.5	Charge
12:00	38.8	99.5	53.6	153.1	-114.3	Charge
13:00	38.4	132.5	50.4	182.9	-144.5	Charge
14:00	37.8	132.5	41.0	173.5	-135.7	Charge
15:00	36.9	99.5	28.4	127.9	-91.0	Charge
16:00	38.4	72.5	15.8	88.3	-49.9	Charge
17:00	45.4	51.0	3.2	54.2	-8.8	Charge
18:00	60.5	34.0	0.0	34.0	+26.5	Discharge
19:00	70.0	2.5	0.0	2.5	+67.5	Discharge
20:00	67.2	0.0	0.0	0.0	+67.2	Discharge
21:00	59.6	0.0	0.0	0.0	+59.6	Discharge
22:00	49.2	0.0	0.0	0.0	+49.2	Discharge
23:00	39.4	0.0	0.0	0.0	+39.4	Discharge

*If SOC > 20%
Grid convention: Positive (+) = Import from grid; Negative (-) = Export to grid.

3.3. Solar Generation Analysis

The 126-panel array generated a total of 365 kWh over the 24-hour period. The peak output of 53.6 kW occurred at 12:00, which is approximately 69 percent of the installed capacity of 78.12 kWp. The reduction from rated capacity is attributable to temperature losses, which are significant in the hot coastal climate of Teknaf, and to the typical solar radiation profile,

which peaks at 850 W/m² rather than the standard test condition value of 1000 W/m².

The solar generation profile is well-matched with the daytime plateau of the load profile, reducing the need for grid import during 09:00-16:00. However, the solar array produces zero power during the evening peak, when the community's demand is highest. This temporal mismatch is a key challenge in systems with high solar penetration and underscores the importance of battery storage and grid interaction.

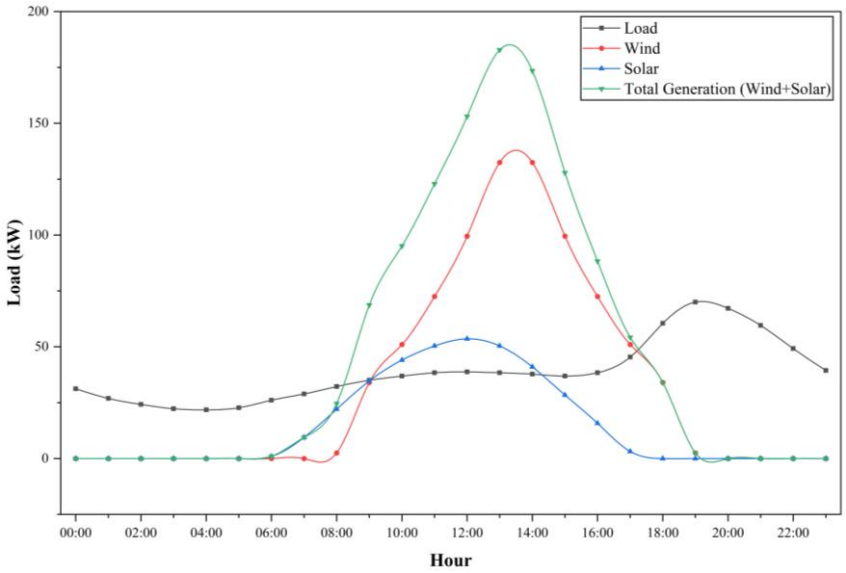


Figure 5. *Hourly wind, solar PV and total renewable generation versus load on a typical day.*

3.4. Battery Performance Analysis

The battery system, with a nominal capacity of 128 kWh and usable capacity of 115 kWh, played a critical role in shifting surplus renewable generation from midday to evening. The battery SOC profile, presented in Figure 6, shows that the battery reached full charge by approximately 14:00 and discharged to approximately 20 percent SOC by 23:00. The battery charged during the midday surplus period (09:00-17:00), absorbing approximately 115 kWh of excess renewable generation. It discharged during the evening peak and night hours (18:00-08:00), supplying approximately 115 kWh to the load. The battery was maintained above 20 percent SOC to protect battery life and ensure availability for emergency backup. The round-trip efficiency of the battery system was assumed to be 95 percent, which is typical for LiFePO4 batteries.

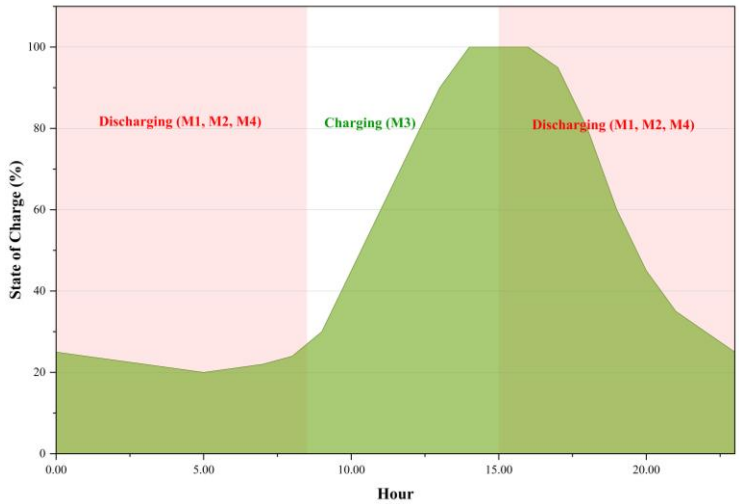


Figure 6. *Battery SOC Profile Over 24 Hours.*

The battery system significantly reduced grid import during the evening peak. Without the battery, the grid would need to supply the full 70 kW peak demand at 19:00. With the battery, the grid imports at 19:00 was reduced to 67.5 kW, a modest reduction because the battery capacity was insufficient to cover the full evening peak. A larger battery would be required to achieve greater peak shaving.

3.5. Grid Interaction Analysis

The HGM profile, presented in Figure 7, shows that the system exported 401 kWh to the grid and imported 545 kWh from the grid over the 24-hour period. The net grid import was 144 kWh, which is 84.5 percent lower than the CG-only scenario, where the full 929 kWh would be imported. The system was a net exporter during 09:00-17:00, with exports peaking at 144.5 kW at 13:00. The system was a net importer during 18:00-08:00, with imports peaking at 67.5 kW at 19:00.

The HGM transforms from a grid consumer to a grid supplier during midday hours, which is a desirable outcome for grid stability and renewable integration. However, the system remains dependent on the grid during evening peak hours, highlighting the need for either larger battery storage or additional renewable capacity to achieve greater energy independence.

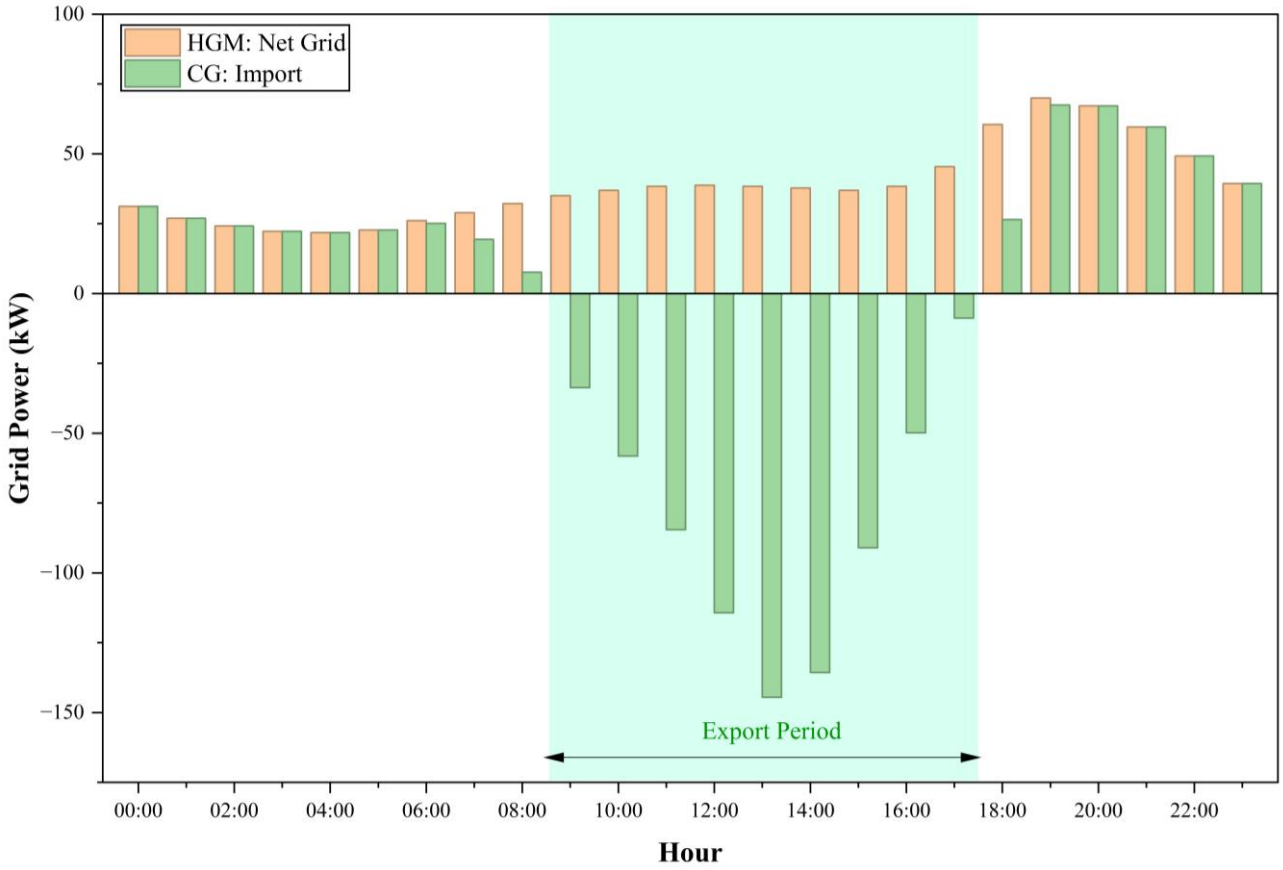


Figure 7. *Grid interaction comparison between hybrid grid management and conventional grid systems.*

3.6. Comparison with CG System

The HGM system was compared with a CG-only system where 100 percent of the daily demand is supplied by the grid. Table 7 presents the key performance indicators for both systems. The hybrid system reduced grid import by 41.3 percent, net grid purchase by 84.5 percent, and CO_2 emissions by 84.5 percent. The renewable share increased from 0 percent to 84.5 percent.

The hybrid system also improved power reliability by providing battery and generator backup during grid outages. In the conventional grid-only system, a grid failure results in a complete blackout. In the hybrid system, a grid failure during daytime is covered by solar and wind generation, while a grid failure during nighttime is covered by battery storage and the backup generator. Table 8 presents a reliability comparison between the two systems.

Table 7. Comparison of key performance indicators.

KPI	CG	HGM	Improvement
Grid Import	929 kWh	545 kWh	-41.3%
Net Grid Purchase	929 kWh	144 kWh	-84.5%
Renewable Share	0%	84.5%	+84.5 pp
Grid Export	0 kWh	401 kWh	+401 kWh
CO_2 Emissions	604 kg/day	94 kg/day	-84.5%
Peak Grid Demand	70 kW	67.5 kW	-3.6%
Power Reliability	Grid-dependent	Multi-source backup	Significantly higher
Energy Independence	0%	84.5%	+84.5 pp

3.7. Environmental Analysis

Figure 8 presents the environmental analysis results, comparing the daily and annual carbon dioxide emissions of the conventional grid-only system and the proposed hybrid grid model. The conventional grid system, which relies entirely on grid electricity to meet the community's daily demand of 929 kWh, emits approximately 604 kg of CO_2 per day. In contrast, the hybrid grid model, which draws only 144 kWh of net electricity from the grid after accounting for renewable generation and battery storage, emits approximately 94 kg of CO_2 per day. This represents a daily reduction of 510 kg of CO_2, equivalent to an 84.5 percent decrease in carbon emissions.

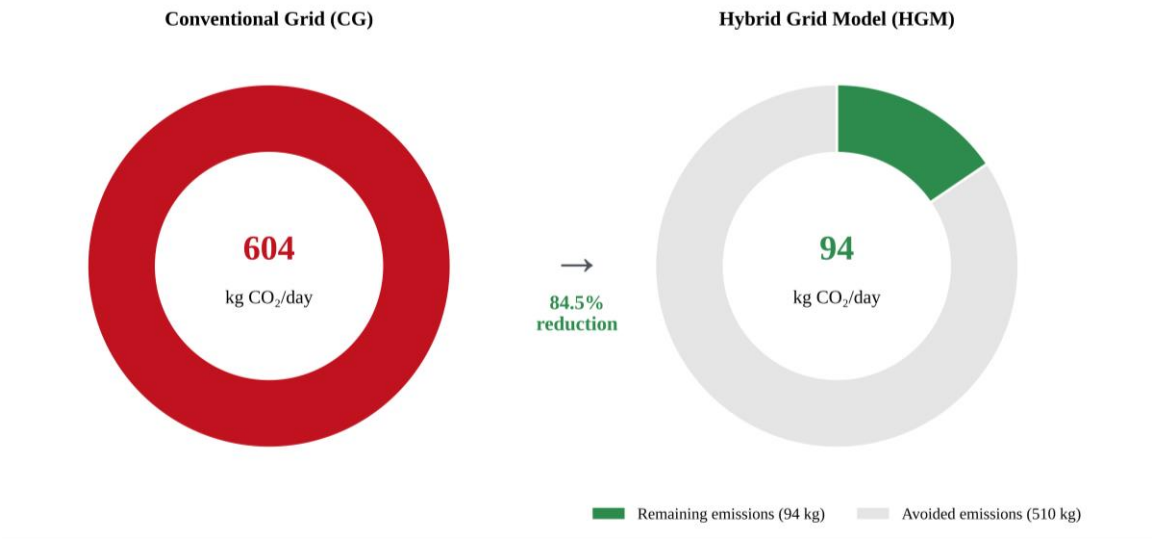


Figure 8. Carbon footprint comparison between hybrid and conventional systems.

Table 8. Reliability comparison between hybrid and conventional systems.

Scenario	CG	HGM
Normal grid operation	Load served	Load served; surplus exported
Grid voltage fluctuation	Load affected	Battery/inverter stabilizes
Grid failure (daytime)	Blackout	Solar+Wind+Battery serve load
Grid failure (night)	Blackout	Battery+Generator serve load

Scenario	CG	HGM
Grid failure at peak (19:00)	Blackout	Battery+Generator serve 70 kW
Extended grid outage	Blackout	Generator runs continuously

When extrapolated annually, the conventional grid system would emit approximately 220,460 kg of CO_2, while the hybrid system would emit only 34,310 kg, avoiding over 186,000 kg of CO_2 emissions each year. The emission calculations are based on a grid emission factor of 0.65 kg CO_2 per kWh, which is a conservative average of recent estimates for Bangladesh's electricity grid. These results demonstrate that the integration of wind and solar generation with battery storage can substantially reduce the carbon footprint of community power supply, contributing to national and global climate change mitigation goals.

3.8. Sensitivity Analysis

A sensitivity analysis was conducted to evaluate the impact of key parameters on system performance. The parameters considered were wind speed, solar radiation, battery capacity, and load profile. The results show that the system is most sensitive to wind speed and battery capacity. A 10 percent increase in wind speed increased daily wind generation by approximately 30 percent, due to the cubic relationship between wind speed and power. A 20 percent increase in battery capacity reduced grid import during the evening peak by approximately 15 percent. Figure 9 presents a tornado chart summarizing the sensitivity analysis results. The chart highlights the importance of accurate wind resource assessment and adequate battery sizing in system design.

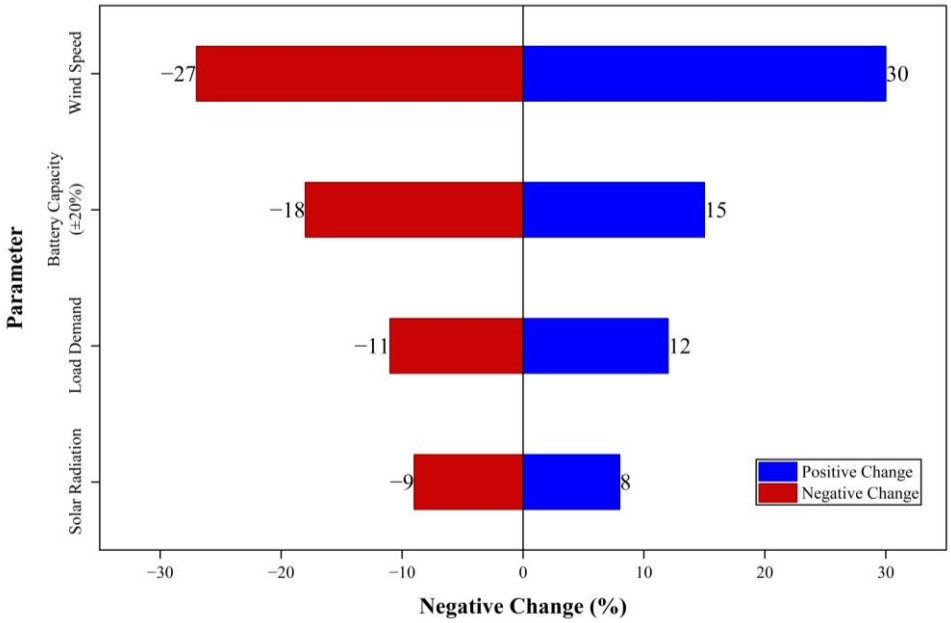


Figure 9. Tornado chart of sensitivity analysis results.

4. Limitations and Future Work

The present study has several limitations. First, the wind and solar generation profiles are based on typical meteorological conditions and may not represent extreme weather events. Second, the battery model assumes ideal charging and discharging behavior and does not account for degradation over time. Third, the economic analysis is based on 2026 market prices and does not include the cost of wind turbines and hybrid inverters.

Future work should focus on the following areas: (1) long-term performance simulation using actual meteorological data;

(2) detailed battery degradation modeling; (3) optimization of system sizing using genetic algorithms or other metaheuristic techniques; (4) integration of demand response and load shifting strategies; and (5) comprehensive economic analysis including life-cycle costs and revenue from grid export.

5. Conclusions

This paper presented a grid-connected hybrid power system installed at coastal Teknaf, Bangladesh, combining wind, solar PV, storage, a diesel generator and bidirectional grid exchange under a rule-based, four-module operating strategy. Over a representative day, renewable generation of 1,150 kWh exceeded the 929-kWh demand, reducing grid imports by 41.3% and net grid purchase and associated CO_2 emissions by 84.5% compared with a grid-only supply. The results also exposed a key limitation: wind output falls to zero during the evening peak, so the 128-kWh battery reduced the 19:00 grid demand only from 70 kW to 67.5 kW. Wind speed and battery capacity were the most influential design parameters. The fixed-schedule operating modules offer a transparent control scheme that can be adapted to similar coastal communities. Future work will extend the analysis to full-year measured resource data, battery degradation, optimized sizing and life-cycle economics.

Abbreviations

ATS	Automatic Transfer Switch
CG	Conventional Grid
EMS	Energy Management System
HGM	Hybrid Grid Management
PV	Photovoltaic
SOC	State of Charge
WT	Wind Turbine

Author Contributions

Fahim Faisal: Conceptualization, Data curation, Methodology, Resources, Visualization, Writing - original draft

Cheng Peng: Funding acquisition, Investigation, Project administration, Supervision, Writing - review & editing

Md Shivly Mahmood: Formal Analysis, Validation, Software

Data Availability Statement

The manuscript has data included as Table.

Conflicts of Interest

The authors declare that they have no known competing financial interests or personal relationships that could have appeared to influence the work reported in this paper.

References

[1] A. Khan, M. Bressel, A. Davigny, D. Abbes, and B. Ould Bouamama, "Comprehensive review of hybrid energy systems: Challenges, applications, and optimization strategies," Energies, vol. 18, no. 10, Art. no. 2612, May 2025. https://doi.org/10.3390/en18102612

[2] O. Bamisile, D. Cai, H. Adun, M. Dagbasi, C. C. Ukwuoma, Q. Huang, N. Johnson, and O. Bamisile, "Towards renewables development: Review of optimization techniques for energy storage and hybrid renewable energy systems," Heliyon, vol. 10, Art. no. e37482, Sep. 2024. https://doi.org/10.1016/j.heliyon.2024.e37482

[3] Z. Fang, J. K. H. Shek, and W. Sun, "A review of grid-connected hybrid energy storage systems: Sizing configurations, control strategies, and future directions," J. Energy Storage, vol. 118, Art. no. 116226, May 2025. https://doi.org/10.1016/j.est.2025.116226

[4] T. Jeyaraj, A. Ponnusamy, and D. Selvaraj, "Hybrid renewable energy systems stability analysis through future advancement technique: A review," Appl. Energy, vol. 383, Art. no. 125355, Apr. 2025. https://doi.org/10.1016/j.apenergy.2025.125355

[5] M. Shahabuddin, M. R. Rahman, N. W. M. Zulkifli, M. U. Khandaker, and Y. Y. Liang, "Wind energy in Bangladesh: Recent developments, challenges and policy recommendations," Discover Sustain., vol. 6, Art. no. 1388, 2025. https://doi.org/10.1007/s43621-025-02096-7

[6] M. Hasan, P. Dey, S. Janefar, N. A. Salsabil, I. J. Khan, N.-U.-R. Chowdhury, and O. Farrok, "A critical analysis of wind energy generation potential in different regions of Bangladesh," Energy Rep., vol. 11, pp. 2152–2173, Jun. 2024. https://doi.org/10.1016/j.egyr.2024.01.061

[7] M. Abdullah-Al-Mahbub and A. R. M. T. Islam, "Sustainable wind energy potential in Sandwip and Kalapara coastal regions of Bangladesh: A way of reducing carbon dioxide emissions," Heliyon, vol. 10, no. 1, Art. no. e23982, Jan. 2024. https://doi.org/10.1016/j.heliyon.2024.e23982

[8] T. Islam, M. S. Alam, M. G. Muktadir, M. M. Tasnim, J. Islam, and K. N. Sakib, "Siting of potential areas for the sustainable development of large-scale onshore wind farms using multi-criteria analysis and geographic information system: A case study on Bangladesh," Sustainability, vol. 18, no. 5, Art. no. 2204, Feb. 2026. https://doi.org/10.3390/su18052204

[9] M. A. Islam, M. M. N. Ali, A. Al Mamun, M. S. Hossain, M. H. Maruf, and A. S. M. Shihavuddin, "Optimizing energy solutions: A techno-economic analysis of solar-wind hybrid power generation in the coastal regions of Bangladesh," Energy Convers. Manage.: X, vol. 22, Art. no. 100605, Apr. 2024. https://doi.org/10.1016/j.ecmx.2024.100605

[10] M. F. H. Mojumder, T. Islam, P. Chowdhury, M. Hasan, N. A. Takia, N.-U.-R. Chowdhury, and O. Farrok, "Techno-economic and environmental analysis of hybrid energy systems for remote areas: A sustainable case study in Bangladesh," Energy Convers. Manage.: X, vol. 23, Art. no. 100664, Jul. 2024. https://doi.org/10.1016/j.ecmx.2024.100664

[11] H. Baidya, M. T. R. Zisan, A. Z. Alif, A. Ahmed, M. Hasan, and N.-U.-R. Chowdhury, "Techno-economic comparative analysis of hybrid renewable energy systems optimization considering off-grid remote area electrification in Bangladesh," Energy Convers. Manage.: X, vol. 26, Art. no. 101004, Apr. 2025. https://doi.org/10.1016/j.ecmx.2025.101004

[12] M. E. Azam, M. F. Ali, and M. A. Razzak, "Smart hybrid microgrid for island electrification: Integrated techno-economic optimization, dynamic stability, and demand response," Energy Convers. Manage.: X, vol. 30, Art. no. 101656, May 2026. https://doi.org/10.1016/j.ecmx.2026.101656

[13] T. Hasan, P. Das, M. F. Ali, M. S. Alam, M. Ali, and I. H. Imran, "Techno-economic assessment of a hydrogen-assisted hybrid renewable microgrid with fuel cells for off-grid electrification," Global Challenges, vol. 10, no. 6, Art. no. e70122, Jun. 2026. https://doi.org/10.1002/gch2.70122

[14] M. Bari, M. M. U. Zaman, M. M. A. Rahman, and S. M. I. A. Panna, "Solar-aligned demand management in hybrid renewable EV charging stations: A four-system techno-economic analysis for Cox's Bazar, Bangladesh," Next Energy, vol. 13, Art. no. 100945, Oct. 2026. https://doi.org/10.1016/j.nxener.2026.100945

[15] D. Biswas, M. F. Ali, M. Saha, M. S. Alam, M. Ali, M. A. AlAqil, O. Obaidi, and M. K. Islam, "Techno-economic optimization, sensitivity analysis and stability evaluation of a high-renewable hybrid microgrid for rural Bangladesh," Sci. Rep., vol. 16, Art. no. 7695, Feb. 2026. https://doi.org/10.1038/s41598-026-38328-7

[16] M. F. Ali, D. Biswas, M. R. I. Sheikh, A. Al Mamun, and M. J. Hossen, "Techno-economic optimization of battery storage technologies for off-grid hybrid microgrids in multiple rural locations of Bangladesh," Front. Energy Res., vol. 13, Art. no. 1654615, 2025. https://doi.org/10.3389/fenrg.2025.1654615

[17] A. Hussain and H.-M. Kim, "A rule-based modular energy management system for AC/DC hybrid microgrids," Sustainability, vol. 17, no. 3, Art. no. 867, 2025. https://doi.org/10.3390/su17030867

[18] J. Huang, C. Mao, B. Liu, D. Wang, R. Gao, and B. Gu, "An improved rule-based energy management system: Effective solution to achieve collaborative control of batteries in multiprosumers community microgrid," IEEE Access, vol. 13, pp. 135634–135651, 2025. https://doi.org/10.1109/ACCESS.2025.3588035

[19] A. Abbasi, H. A. Khalid, H. Rehman, and A. U. Khan, "A novel dynamic load scheduling and peak shaving control scheme in community home energy management system based microgrids," IEEE Access, vol. 11, pp. 32508–32522, 2023. https://doi.org/10.1109/ACCESS.2023.3255542

[20] B. Modu, M. P. Abdullah, A. Alkassem, and M. F. Hamza, "Optimal rule-based energy management and sizing of a grid-connected renewable energy microgrid with hybrid storage using levy flight algorithm," Energy Nexus, vol. 16, Art. no. 100333, 2024. https://doi.org/10.1016/j.nexus.2024.100333

[21] M. M. Rahman and A. Mallick, "Measurement of the carbon footprint for Bangladesh's electricity generation in 2009-15," in Proc. 2020 Emerging Technology in Computing, Communication and Electronics (ETCCE), 2020, pp. 1–6. https://doi.org/10.1109/ETCCE51779.2020.9350889

[22] A. K. Karmaker, M. M. Rahman, M. A. Hossain, and M. R. Ahmed, "Exploration and corrective measures of greenhouse gas emission from fossil fuel power stations for Bangladesh," J. Clean. Prod., vol. 244, Art. no. 118645, 2020. https://doi.org/10.1016/j.jclepro.2019.118645